Estimating interfacial thermal conductivity in metamaterials through heat flux mapping

Fatih M. Canbazoglu, Krishna P. Vemuri, and Prabhakar R. Bandaru

Citation: Applied Physics Letters **106**, 143904 (2015); doi: 10.1063/1.4917344
View online: http://dx.doi.org/10.1063/1.4917344
View Table of Contents: http://scitation.aip.org/content/aip/journal/apl/106/14?ver=pdfcov
Published by the AIP Publishing

APPLIED PHYSICS LETTERS **106**, 143904 (2015)

Estimating interfacial thermal conductivity in metamaterials through heat flux mapping

Fatih M. Canbazoglu, Krishna P. Vemuri, and Prabhakar R. Bandaru[a)]
Department of Mechanical and Aerospace Engineering, University of California, San Diego, La Jolla, California 92093, USA

(Received 31 January 2015; accepted 26 March 2015; published online 8 April 2015)

The variability of the thickness as well as the thermal conductivity of interfaces in composites may significantly influence thermal transport characteristics and the notion of a metamaterial as an effective medium. The consequent modulations of the heat flux passage are analytically and experimentally examined through a non-contact methodology using radiative imaging, on a model anisotropic thermal metamaterial. It was indicated that a lower Al layer/silver interfacial epoxy ratio of ∼25 compared to that of a Al layer/alumina interfacial epoxy (of ∼39) contributes to a smaller deviation of the heat flux bending angle. © *2015 AIP Publishing LLC*.
[http://dx.doi.org/10.1063/1.4917344]

Metamaterials are often synthesized through optimized arrangement or layering of isotropic materials and should ideally can be treated as an effective medium.[1,2] Such a requirement intrinsically assumes that the interfaces between the constituents are not relevant in determining the overall characteristics of the metamaterial. For example, a wavelength/structural feature ratio of 10:1 has often been considered[3] as one criterion for an effective medium in the case of electromagnetic interactions. However, for the case of diffusive transport,[4] as would be the case for thermal metamaterials, the criteria may be less well defined.[5] In this paper, we consider the possible effects of interfaces in modulating heat transfer.[6,7] We use a non-contact methodology, based on radiative heat imaging, for probing the role of the interfacial thickness as well as its thermal conductivity in regulating heat flux through composite media.[8]

At the very outset, the interfacial thermal resistance[9] (R_{int}) is defined for an area, A, through $R_{int}A = l_{int}/\kappa_{int}$, where l_{int} and κ_{int} are the effective thickness and thermal conductivity of the interface, respectively (Fig. 1(a)). In practical construction of the composite, there is an intrinsic variability in both the l_{int} and the κ_{int}, which could play a significant role in establishing a true metric of the thermal boundary resistance (TBR).[10] We seek to understand the modulation of a specific functionality in thermal metamaterials,[5,11] i.e., the variation of the heat flux bending, due to such physical parameter fluctuations intrinsic to an interface.

We have previously shown[5] that assembling a composite of two alternating materials, with isotropic thermal conductivity (of κ_1 and κ_2, say, with $\kappa_1 > \kappa_2$, Fig. 1(a)), and rotating the layers (say, by an angle θ as in Fig. 1(b)), with respect to a horizontal thermal gradient direction may cause the heat flux to bend by a specific angle: ϕ. In the earlier treatment,[5] the interfacial effect was not considered under a proposed effective thermal medium (ETM) approach. It was shown that the difference (ΔT) between the temperature obtained at a given point—(i) obtained through assuming a linear temperature gradient across the composite (equivalent to defining an effective thermal conductivity for the composite), and (ii) through considering temperature variation across the individual layers, could be drastically reduced, through a small κ_1/κ_2 ratio as well as a large number of layers (n) in the composite. Consequently, the angle of heat flux bending was derived to be

$$\phi = \tan^{-1}\left[\frac{(-1+c)\cos(\theta)\sin(\theta)}{\cos^2(\theta)+c\,\sin^2(\theta)}\right] \text{ with } c = \frac{\left(1+\frac{\kappa_1}{\kappa_2}\right)^2}{4\,\frac{\kappa_1}{\kappa_2}}. \tag{1}$$

Both positive and negative values of the ϕ, corresponding to the upwards/downwards bending of the heat flux, were also demonstrated.[12,13] However, in the earlier study, (a) the two layers were assumed to be of equal thickness and (b) interfacial effects were ignored. As an example of the construction of an ETM, we now consider a composite constituted from Al layers ($\kappa_1 = \kappa_{Al}$) joined together with epoxy ($\kappa_2 = \kappa_{int}$), which serves as the interfacial (*int*) material. When both l_{int} and κ_{int} are considered, the heat flux bending angle would be modified to $\phi_{\rm int}$ (see Sec. I of the supplementary material[16] for further details of the derivation), to a value

$$\begin{aligned}
\phi_{int} &= \tan^{-1}\left[\frac{(-a+b)\cos(\theta)\sin(\theta)}{a\,\cos^2(\theta)+b\,\sin^2(\theta)}\right],\\
a &= (l_{Al}+l_{int})^2\left(\frac{\kappa_{Al}}{\kappa_{int}}\right),\\
b &= (l_{Al})^2\left(\frac{\kappa_{Al}}{\kappa_{int}}\right)+l_{Al}l_{int}\left(\frac{\kappa_{Al}}{\kappa_{int}}\right)^2+l_{Al}l_{int}+(l_{int})^2\left(\frac{\kappa_{Al}}{\kappa_{int}}\right).
\end{aligned} \tag{2}$$

It is evident then that the presence and consideration of the interface may significantly alter the bending angle. Consequently, the experimental observation of the heat flux could yield insights into interfacial characteristics.

The experiments were carried out through assembling an even number ($n = 34$) of thin layers of aluminum (assuming

[a)]Electronic mail: pbandaru@ucsd.edu

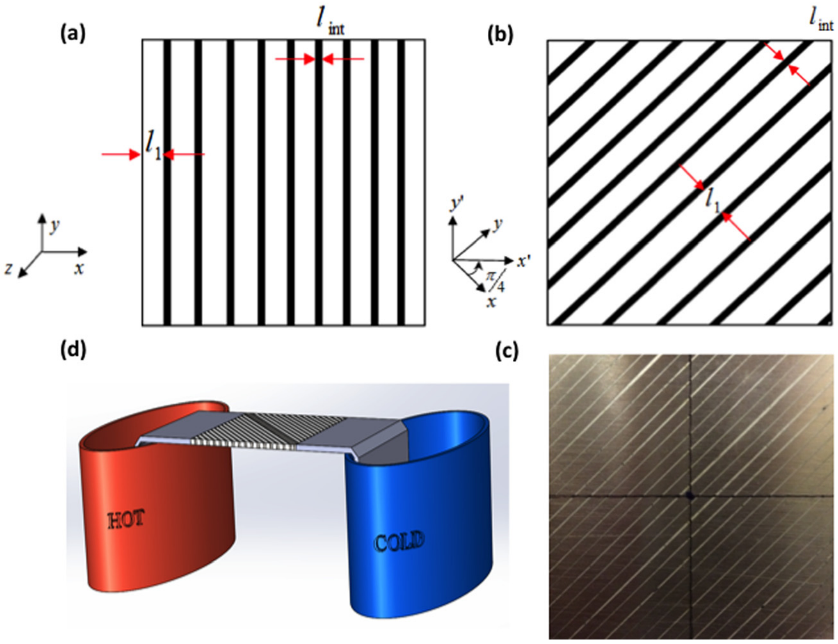

FIG. 1. (a) A multilayered composite/metamaterial may be fabricated through joining isotropic material (of thickness: l_1 and thermal conductivity: κ_1) and an interfacial epoxy (of thickness: l_{int} and thermal conductivity: κ_{int}), (b) anisotropy can be induced in the composite through rotating the layers of the composite by an angle θ, leading to a heat flux bending, which would be sensitive to the l_{int} and κ_{int}, (c) an experimental sample composed of aluminum layers joined by alumina epoxy, with the layers oriented at $\theta = 45°$, (d) the composite sample was placed in a temperature gradient ($\sim$80 K sustained over a length of $\sim$9 cm), facilitated through hot and cold water bath reservoirs.

an isotropic $\kappa_{Al} = 205$ W/m K and $l_{Al} = 0.17$ cm) which were joined together using two different types of thermally conductive adhesive, i.e., (i) an alumina epoxy—from Arctic Silver, Inc., specified by the manufacturer with a thermal conductivity in the range of 0.5–7.5 W/m K and (ii) a silver epoxy—Arctic Silver, Inc., specified with a thermal conductivity >7.5 W/m K, respectively. The samples were fabricated in a square geometry with a length and width of 5 cm each and have a thickness of $\sim$0.3 cm, implying a large length/width to thickness aspect ratio (of $\sim$17) and the consideration of the heat flux in a two-dimensional ETM plane. The joining process naturally incorporates variability in both the l_{int} and κ_{int}. The metamaterial assembly was oriented at an angle $\theta = 45°$, as indicated in Fig. 1(c), with respect to a horizontal temperature gradient of $\sim$80 K ($T_{hot} = 100\,°$C and $T_{cold} = 22\,°$C) (Fig. 1(d)). The hot and cold-temperatures were maintained using water baths of large heat capacity. The steady state temperature profiles were obtained through using an infra-red (IR) camera (FLIR 320), with a spatial resolution/spot size of $\sim$385 μm, a temperature resolution of $\sim$0.5 K, and a spectral range of 3–5 μm. For obtaining an enhanced signal, the top surfaces of the samples of Fig. 1(c) were painted with a thin layer of black acrylic paint (DA67: DecoArt Americana, Ebony Black, of emissivity $\sim$0.93 in the given spectral range). The results of the imaging are indicated through the temperature recordings in Fig. 2(a)—for the silver epoxy and Fig. 2(b)—for the alumina epoxy. While the heat flux lines would not be oriented in the temperature gradient direction, due to the anisotropy in the composite/metamaterial, the bending of the flux is clearly evident in the considered figures. Given that the typical interface thickness to the Al layer thickness ratio was determined to be of the order of 0.1 (as also discussed later with reference to Fig. 3), it is remarkable that a considerable heat flux modulation is being observed. The relative spacing of the isotherms in the composite would be a function of the κ_{Al}/κ_{int} as well as the l_{Al}/l_{int} ratio, as may be understood by reference to a limiting case where a larger material/interface thermal conductivity ratio could yield further compression of the isotherms towards the center of the composite.

The spot size enabled by the IR camera yielded a matrix (130 × 130 points) of temperature readings: $T(x,y)$ over the sample area. At steady state and in the absence of losses, the heat conduction equation for a given heat flux q_i in an anisotropic composite would be

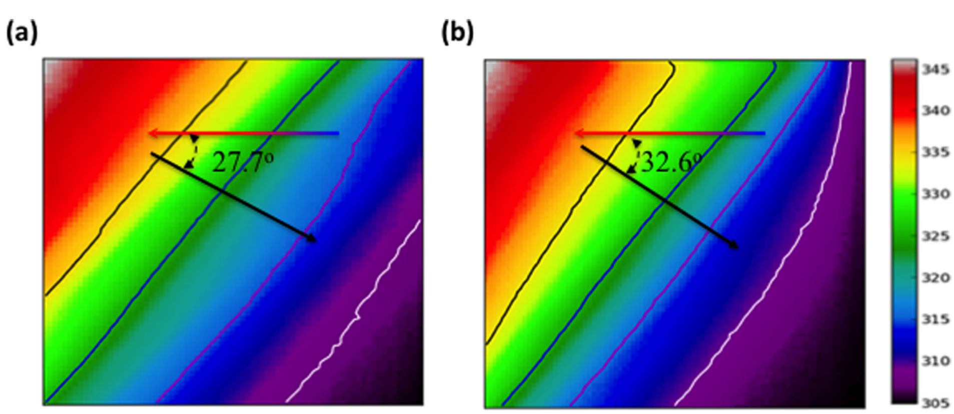

FIG. 2. The steady state transport of heat, as obtained by infra-red imaging, through (a) aluminum layer-silver epoxy and (b) aluminum layer-alumina epoxy, joined composites. The scale bar indicates the temperatures (in K). Typical isothermal contours are at 335 K, 325 K, 315 K, and 308 K, from the left to right. The angles refer to the direction of *net* heat flux bending with respect to a horizontally applied temperature gradient.

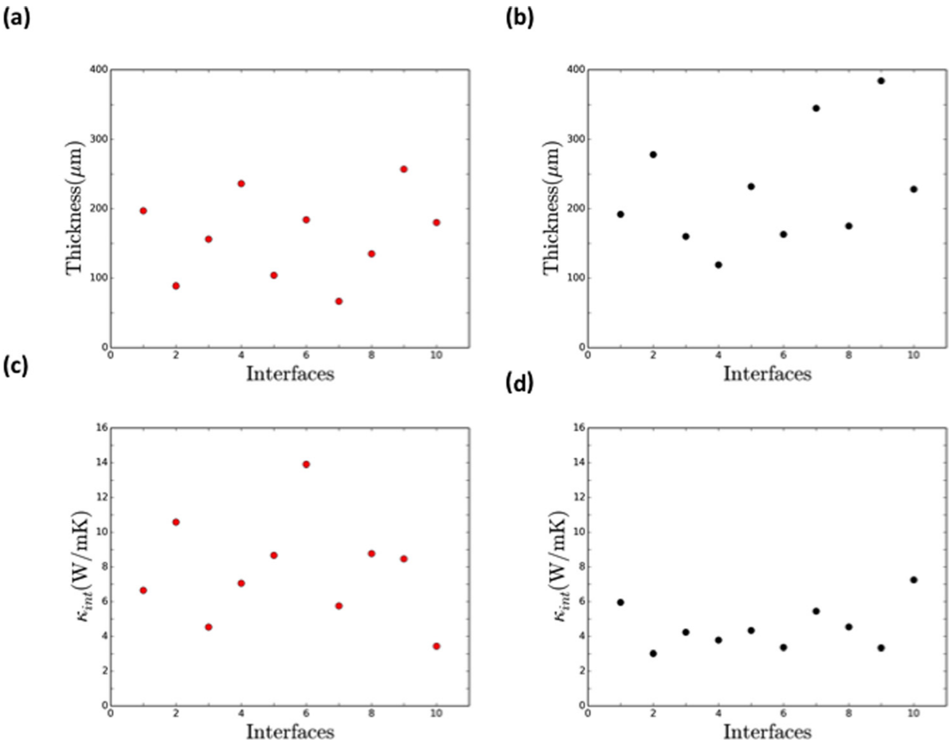

FIG. 3. The measured interfacial thickness variation for the (a) aluminum layer-silver epoxy and (b) aluminum layer-alumina epoxy, joined composites. The estimated thermal conductivity variation for the (c) aluminum layer-silver epoxy, and (d) aluminum layer-alumina epoxy, joined composites.

$$\nabla \cdot q_i = \nabla \cdot (\kappa_{ij} \nabla T_j) = \kappa_{xx} \frac{\partial^2 T(x,y)}{\partial x^2} + 2\,\kappa_{xy} \frac{\partial^2 T(x,y)}{\partial x \partial y} + \kappa_{yy} \frac{\partial^2 T(x,y)}{\partial y^2}. \tag{3}$$

In the above relation, the κ_{xx}, κ_{yy}, and κ_{xy} are all functions of the κ_{Al}, l_{Al}, κ_{int}, l_{int}, and the θ (see supplementary material[16]). As all the other variables, except the l_{int} and the κ_{int}, are known the solution of Eq. (3) would determine the interfacial characteristics.

Initially, the horizontal and vertical temperature gradients were obtained through averaging the temperature readings over a length of 5 points. Such a distance of 0.1925 cm ($=385\,\mu$m $\times$ 5) was chosen to ensure that the interface between the Al layers was always sampled, i.e., as the $l_{Al} = 0.17$ cm. Subsequently, the second derivatives: $\frac{\partial^2 T(x,y)}{\partial x^2}$, $\frac{\partial^2 T(x,y)}{\partial y^2}$, and $\frac{\partial^2 T(x,y)}{\partial x \partial y}\left(= \frac{\partial^2 T(x,y)}{\partial y \partial x}\right)$ were computed through a second-order forward difference methodology (also see Sec. II of the supplementary material[16]).

Then, the location of each interface on the line transverse to that along which the temperatures were recorded, and the corresponding l_{int} were measured through scanning electron microscopy (SEM) based imaging. A representative variation of the l_{int} is indicated for ten consecutive interfaces in Figs. 3(a) and 3(b), for the Al layers joined by silver and alumina epoxy, respectively. It was noted that the interface averaged $l_{int,\ alumina}$ was $203 \pm 81\,\mu$m and the $l_{int,silver}$ was $209 \pm 114\,\mu$m. Subsequently, Eq. (3) was solved, using the l_{int} values, obtained through the SEM imaging, to yield the κ_{int}. The variation of the $\kappa_{int,\ silver}$ along the ten interfaces is indicated in Fig. 3(c), with a range of 3.4–13.9 W/m K (averaged over all the interfaces to be 8.3 ± 3.4 W/m K) and that for $\kappa_{int,\ alumina}$ in Fig. 3(d)—with a range of 3.0– 7.3 W/m K (averaged over all the interfaces to be 5.2 ± 3.7 W/m K). Such variation in both the l_{int} and the κ_{int} is representative of practical interfaces, and the latter is be contrasted to typical manufacturer specifications of the epoxy thermal conductivity (i.e., in the range of 0.5–7.5 W/m K for the alumina epoxy and >7.5 W/m K for the silver epoxy). The estimates of the interfacial resistance,[7,14,15] $R_{int}A$ ($=l_{int}/\kappa_{int}$) range from 0.3–13.4 $\times 10^{-5}$ m^2 K/W and 1.0– 4.4 $\times 10^{-5}$ m^2 K/W for the Al layer-alumina epoxy and the Al layer-silver epoxy constituted composites, respectively.

For obtaining the average values of the interfacial parameters, Eq. (2) was used to plot the $\phi_{\rm int}$ as a function of the l_{int} and is shown in Fig. 4, with individual curves in the graph correspond to varying κ_{Al}/κ_{int} values. Generally, the $\phi_{\rm int}$ shows an initial linear variation followed by a saturation behavior at larger values of the l_{int}. Intuitively, large l_{int}

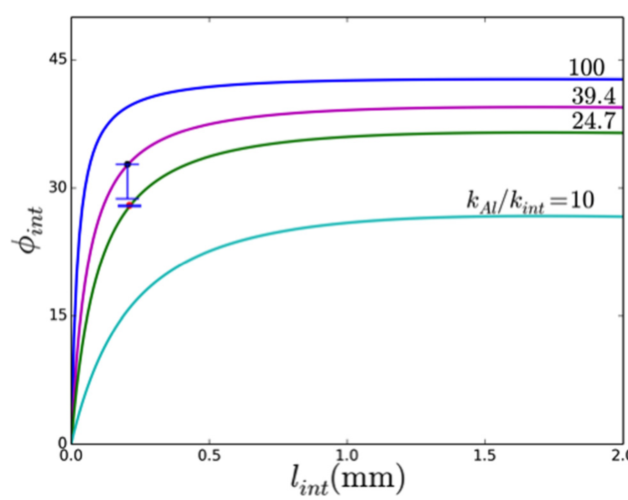

FIG. 4. The heat flux bending angle (ϕ_{int}) variation with the interfacial thickness ($l_{\rm int}$) as a function of the κ_{Al}/κ_{int} ratio, plotted per Eq. (2) and with $\theta = 45°$. The marked points correspond to the determined $\kappa_{Al}/\kappa_{int,\ alumina}$ ratio of ~39.4 and a $\kappa_{Al}/\kappa_{int,\ silver}$ ratio of ~24.7.

TABLE I. The net change of the observed heat flux bending angle ($=d\phi_{\rm int}$) due to the individual variation in the interfacial thickness ($=\partial l_{int}$) and the interfacial thermal conductivity ($=\partial\kappa_{int}$) for the aluminum layer-silver epoxy and aluminum layer-alumina epoxy, joined composites.

	$\frac{\partial\phi_{\rm int}}{\partial\kappa_{\rm int}}$	$d\kappa_{\rm int}$(W/m K)	$\frac{\partial\phi_{\rm int}}{\partial l_{\rm int}}$	$dl_{\rm int}$(μm)	$d\phi_{\rm int}$
Al-silver epoxy	−1.5	3.4	41.8	114	-0.3^0
Al-alumina epoxy	−1.9	3.7	36.3	81	-4.1^0

corresponds to a situation where the heat flux preferentially follows the higher thermal conductivity Al layer and a concomitant decreasing influence of the interface. Equivalently, a similar behavior would be expected for a very large κ_{Al}/κ_{int} ratio, and the $\phi_{\rm int}$ would saturate at an angle of $(90-\theta)$.[5] From $\kappa_{Al} = 205$ W/m K and the obtained average values of the $\kappa_{int,\,silver}$ and the $\kappa_{int,\,alumina}$ (8.3 W/m K and 5.2 W/m K, respectively), the $\phi_{\rm int}$ was estimated to be 27.7° and 32.6°, for the two adhesives, respectively. These values are superposed on the plots of Fig. 4 with a $\kappa_{Al}/\kappa_{int,\,alumina}$ ratio of ~39.4 and a $\kappa_{Al}/\kappa_{int,\,silver}$ ratio of ~24.7. These angles correspond to the extent of heat flux bending given through the $\phi_{\rm int}$ and consider the interfacial effects and variations.

The change in the $\phi_{\rm int}$ ($=d\phi_{\rm int}$) due to the variation in the l_{int} ($=\partial l_{int}$) and the κ_{int} ($=\partial\kappa_{int}$) can be understood through a relation of the form

$$d\phi_{int} = \frac{\partial\phi_{int}}{\partial\kappa_{int}}d\kappa_{int} + \frac{\partial\phi_{int}}{\partial l_{int}}dl_{int}. \quad (4)$$

The partial derivatives were computed from Eq. (2) and the results of the estimation, with respect to the variation of the heat flux bending angle are indicated in Table I. It is apparent that a lower $\kappa_{Al}/\kappa_{int,silver}$ ratio of ~25 compared to the of $\kappa_{Al}/\kappa_{int,alumina}$ of ~39, contributes to the smaller deviation of the heat flux bending angle. It is also pertinent to note that the interfacial conductivity variation may play a larger role compared to the thickness variation, due to the dominance of the first term in Eq. (4). As there would always be such thickness and thermal conductivity variation, the degree to which a thermal metamaterial can be approximated as an effective thermal medium should be carefully considered.

In summary, our work has indicated that the variation of the interfacial parameters is crucial for composite and metamaterial layers joined by adhesives with a large $\kappa_{material}/\kappa_{adhesive}$ ratio. We have proposed a non-contact method, based on the amount of heat flux bending, to deduce the interface characteristics and deviations from the predicted values.

This work was partially supported by a grant (CMMI 1246800) from the National Science Foundation (NSF). We would like to acknowledge Kenneth Duff for his help with the composite manufacture and S. Yavuz for assistance with Scanning Electron Microscopy imaging.

[1]M. Kadic, T. Bueckmann, R. Schittny, and M. Wegener, Rep. Prog. Phys. **76**, 126501 (2013).
[2]D. R. Smith, J. B. Pendry, and M. C. K. Wiltshire, Science **305**, 788 (2004).
[3]J. B. Pendry, A. J. Holden, D. J. Robbins, and W. J. Stewart, IEEE Trans. Microw. Theory Tech. **47**, 2075 (1999).
[4]A. A. Joshi and A. Majumdar, J. Appl. Phys. **74**, 31 (1993).
[5]K. P. Vemuri and P. R. Bandaru, Appl. Phys. Lett. **103**, 133111 (2013).
[6]M. P. Harmer, Science **332**, 182 (2011).
[7]B.-W. Kim, S.-H. Park, R. S. Kapadia, and P. R. Bandaru, Appl. Phys. Lett. **102**, 243105 (2013).
[8]D. G. Cahill, W. K. Ford, K. E. Goodson, G. D. Mahan, A. Majumdar, H. J. Maris, R. Merlin, and S. R. Phillpot, J. Appl. Phys. **93**, 793 (2003).
[9]E. T. Swartz and R. O. Pohl, Rev. Mod. Phys. **61**, 605 (1989).
[10]R. S. Prasher, Proc. IEEE **94**, 1571 (2006).
[11]S. Narayana and Y. Sato, Phys. Rev. Lett. **108**, 214303 (2012).
[12]T. Yang, K. P. Vemuri, and P. R. Bandaru, Appl. Phys. Lett. **105**, 083908 (2014).
[13]K. P. Vemuri, F. M. Canbazoglu, and P. R. Bandaru, Appl. Phys. Lett. **105**, 193904 (2014).
[14]C.-W. Nan, R. Birringer, D. R. Clarke, and H. Gleiter, J. Appl. Phys. **81**, 6692 (1997).
[15]S. T. Huxtable, D. G. Cahill, S. Shenogin, L. Xue, R. Ozisik, P. Barone, M. Usrey, M. S. Strano, G. Siddons, M. Shim, and P. Keblinski, Nat. Mater. **2**, 731 (2003).
[16]See supplementary material at http://dx.doi.org/10.1063/1.4917344 for (i) derivation of the heat flux bending angle considering the effects of interfacial thickness and thermal conductivity and (ii) computation of the spatial temperature derivatives.